ARMY RESEARCH LABORATORY

Numerical Investigation of the External Propulsion Ram Accelerator

Michael J. Nusca

ARL-TR-920 January 1996

NOTICES

Destroy this report when it is no longer needed. DO NOT return it to the originator.

Additional copies of this report may be obtained from the National Technical Information Service, U.S. Department of Commerce, 5285 Port Royal Road, Springfield, VA 22161.

The findings of this report are not to be construed as an official Department of the Army position, unless so designated by other authorized documents.

The use of trade names or manufacturers' names in this report does not constitute indorsement of any commercial product.

REPORT DOCUMENTATION PAGE

Form Approved
OMB No. 0704-0188

1. AGENCY USE ONLY *(Leave blank)*	2. REPORT DATE	3. REPORT TYPE AND DATES COVERED
	January 1996	Final, April–December 1994

4. TITLE AND SUBTITLE

Numerical Investigation of the External Propulsion Ram Accelerator

5. FUNDING NUMBERS

PR: 1L162618A1FL

6. AUTHOR(S)

Michael J. Nusca

7. PERFORMING ORGANIZATION NAME(S) AND ADDRESS(ES)

U.S. Army Research Laboratory
ATTN: AMSRL-WT-PA
Aberdeen Proving Ground, MD 21005-5066

8. PERFORMING ORGANIZATION REPORT NUMBER

ARL-TR-920

9. SPONSORING/MONITORING AGENCY NAME(S) AND ADDRESS(ES)

10. SPONSORING/MONITORING AGENCY REPORT NUMBER

11. SUPPLEMENTARY NOTES

12a. DISTRIBUTION/AVAILABILITY STATEMENT

Approved for public release; distribution is unlimited.

12b. DISTRIBUTION CODE

13. ABSTRACT *(Maximum 200 words)*

Computations of the hypersonic flow of a combustible mixture over a projectile are presented. A projectile of maximum 32-mm diameter is launched into a 120-mm-diameter gun tube at Mach numbers of 6–10. The gun tube is sealed at both ends with diaphragms and filled with a fuel-rich methane/oxygen/nitrogen mixture at an initial pressure of 50 atm and temperature of 300 K. Combustion is established on the projectile by a small forward-facing step positioned on the projectile. Results demonstrate that step heights of 0.5, 1, and 1.5 mm cause detonation of the mixture at the step with sustained combustion over the afterbody and base of the projectile. The interaction between the bow and shock from the conical forebody and the detached shock-detonation on the forward-facing step, positioned at the forebody-afterbody junction, results in confinement of a combustion layer around the projectile afterbody. The resulting high pressure and temperature combustion products, which are confined to this layer, are expanded into the projectile wake, generating thrust.

14. SUBJECT TERMS

Navier-Stokes, computational fluid dynamics, reacting flow, detonation, kinetics, ram accelerator, external propulsion

15. NUMBER OF PAGES

26

16. PRICE CODE

17. SECURITY CLASSIFICATION OF REPORT	18. SECURITY CLASSIFICATION OF THIS PAGE	19. SECURITY CLASSIFICATION OF ABSTRACT	20. LIMITATION OF ABSTRACT
UNCLASSIFIED	UNCLASSIFIED	UNCLASSIFIED	UL

INTENTIONALLY LEFT BLANK.

ACKNOWLEDGMENTS

Mr. D. Kruczynski and Mr. A. Horst, U.S. Army Research Laboratory, have supported numerical simulation for the HIRAM project since its inception and have contributed to this work through various technical discussions. Drs. S. Palaniswamy and S. Chakravarthy, Rockwell Science Center, provided numerous points of technical assistance with the USA-RG code and without whose help this work would not have been possible. Dr. J. Rom (Technion, Israel) is acknowledged for technical consultation with regards to the external accelerator and for requesting that the computational fluid dynamics (CFD) computations be completed.

INTENTIONALLY LEFT BLANK.

TABLE OF CONTENTS

INTENTIONALLY LEFT BLANK.

LIST OF FIGURES

INTENTIONALLY LEFT BLANK.

1. INTRODUCTION

The external propulsion accelerator was proposed by Rom (1990) and certain operating characteristics were presented by Rom and Kivity (1988) and Rom and Avital (1992). The external propulsion accelerator was proposed for development based on the successful development of the ram accelerator by Hertzberg and colleagues at the University of Washington (Hertzberg, Bruckner, and Bogdanoff 1988). Several issues related to the theory and operation of the external propulsion accelerator are: 1) the establishment of combustion by a small step on the projectile and the possibility of flame quenching on the projectile afterbody, 2) the generation of enough thrust to counter the drag produced by the step, 3) centering of the projectile within the accelerator tube at launch and the aeroballistic stability during flight through the tube, and 4) potential advantages of the external propulsion accelerator as compared to the ram accelerator. This report addresses the first two issues and leaves the remaining issue for further study.

In the ram accelerator, a projectile and obturator are injected at supersonic velocity into a stationary tube filled with a pressurized mixture of hydrocarbon, oxidizer, and inert gases. Flow stagnation on the obturator initiates combustion of the mixture. A system of shock waves generated on the projectile and reflected from the accelerator tube wall, in conjunction with viscous heating, sustains combustion. The resulting energy release, which travels with the projectile, also generates high pressures that impart thrust to the projectile. The U.S. Army Research Laboratory (ARL) ram accelerator system uses a 120-mm (bore diameter) tube that is modeled after the 38-mm system at the University of Washington (Hertzberg, Bruckner, and Bogdanoff 1988). Numerical simulation conducted at ARL using finite-rate chemical kinetics has been used to investigate this flow field. Numerical results are used to visualize the flow field, predict effects of variation in system parameters, and predict projectile in-bore velocity (Nusca 1994). Ram acceleration (30-mm and 90-mm bore) has also been demonstrated at the Institute of St. Louis (ISL) in France (Giraud, Legendre, and Simon 1991; Smeets et al. 1994).

Unlike the ram accelerator, thrust for the external propulsion accelerator is generated by combustion that is initiated by a normal shock wave generated on the projectile body using a ramp or forward-facing step. Since the projectile is subcaliber, the process is independent of the tube wall (except that the tube contains the pressurized mixture). There are potentially difficult design issues such as the ability to initiate and stabilize the combustion front on the projectile in such a way that positive thrust can be generated. The step that initiates combustion also produces a drag component. Previous studies (Rom and Kivity 1988; Rom and Avital 1992) indicated that if a relatively small forward-facing step on the projectile

shoulder (i.e., the forebody-afterbody junction) is able to induce a detonation wave and a sustained combustion front, then reasonable thrust levels may be achieved.

The present investigation examines the ability of a small forward-facing step to ignite the premixed fuel/oxidizer mixture flowing at hypersonic speeds over the projectile (due to projectile movement). The flowfield and combustion front generated by the interaction of the bow shock from the projectile nose and the detonation wave generated by the step are investigated. This interaction results in the confinement of a high pressure and temperature region below a contact surface (see Figure 1). This region, located between the projectile body and the contact surface, acts like the combustion chamber of an engine. However, in this case, the contact surface acts as the "engine cowling" without a structural boundary. The high temperature and pressure combustion products are then expanded over the afterbody of the projectile to produce thrust. The flowfield, with chemical reactions, is studied in detail using the numerical solution of the Reynolds Averaged Navier-Stokes (RANS) equations, including the equations for chemical species and finite-rate kinetics.

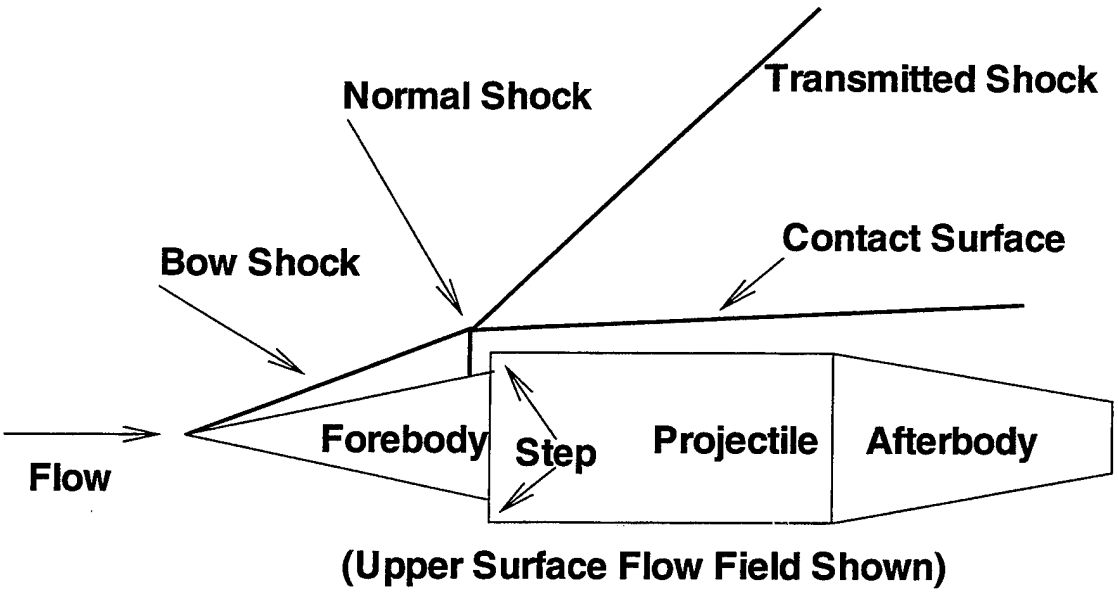

Figure 1. Schematic of projectile and reacting flowfield.

The present investigation uses the solution of the RANS equations for flows with chemical processes adapted for the ram accelerator configuration at ARL by Nusca (1991, 1993, 1994) and Kruczynski and Nusca (1992) and is summarized in this report. In these calculations, the same mixture of CH_4, O_2, and N_2 selected at ARL for the ram accelerator firings is used. The chemical reaction mechanism for this

mixture, used in the calculations for the ARL ram accelerator, has yielded good results when compared with experimental data (Nusca 1994). Although the combustion conditions in the case of the external propulsion accelerator are different from those in the ram accelerator (i.e., scale of the projectile and method of ignition), it has been assumed in this report that by using the same mixture with the same kinetics model, plausible results can be achieved for the external propulsion accelerator as well. This report presents calculations for the effects of step height and projectile Mach number, using several projectile geometries, on the combustion process and resulting thrust. These calculations are also used to study the flow ahead of the forward-facing step, including the formation of a combustion/detonation front.

2. REACTING FLOW MODEL

Computational fluid dynamics (CFD) flow simulations for the ram accelerator projectile were performed at ARL using the Rockwell Science Center USA-RG (Unified Solution Algorithm Real Gas) code (Chakravarthy et al. 1985; Palaniswamy and Chakravarthy 1989; Palaniswamy, Ota, and Chakravarthy 1991). Nusca (1991, 1993, 1994) and Kruczynski and Nusca (1992) used this code successfully at ARL for simulation of a full-bore 120-mm ram accelerator projectile. This CFD code solves the full, 3-D, unsteady RANS equations, including equations for chemical kinetics (finite-rate and equilibrium). These partial differential equations are cast in conservation form and converted to algebraic equations using an upwind finite-volume formulation. Solution takes place on a mesh of nodes distributed in a zonal fashion around the projectile and throughout the flowfield such that sharp geometric corners and other details are accurately represented. The conservation law form of the equations assures that the end states of regions of discontinuity (shocks, detonations, deflagrations) are physically correct even when smeared over a few computational cells. The total variation diminishing (TVD) technique is employed to discretize inertia terms of the conservation equations, while the viscous terms are evaluated using an unbiased stencil. Flux computations across cell boundaries are based on Roe's scheme for hyperbolic equations (Roe 1981). Third-order spatial accuracy can be maintained in regions of the flow field with continuous variation while slope limiting, used near large flow gradients, reduces the accuracy locally to avoid spurious oscillations.

The RANS equations for 2-D/axisymmetric reacting flow (N species mixture) are written in the following conservation form (Palaniswamy and Chakravarthy 1989) for dependent variables of energy (e), density (ρ), axial and radial momentum flux (ρu, ρv), and species flux ($\rho\sigma$).

$$\frac{\partial W}{\partial t} + \frac{\partial (F_1 - G_1)}{\partial x} + \frac{\partial (F_2 - G_2)}{\partial y} + \frac{\alpha (F_2 - G_2)}{y} = \Omega$$

$$W = (e, \rho, \rho u, \rho v, \rho\sigma_1, \ldots, \rho\sigma_{N-1})$$

$$F_1 = \left((e + p)u, \rho u, \rho u^2 + p, \rho uv, \rho u\sigma_1, \ldots, \rho u\sigma_{N-1}\right)$$

$$F_2 = \left((e + p)v, \rho v, \rho vu, \rho v^2 + p, \rho v\sigma_1, \ldots, \rho v\sigma_{N-1}\right)$$

$$G_1 = \left(\kappa_m \frac{\partial T}{\partial x} + \sum_i \rho D(h_i - h_N)\frac{\partial \sigma_i}{\partial x} + u\tau_{xx} + v\tau_{xy}, 0, \tau_{xx}, \tau_{xy}, \rho D\frac{\partial \sigma_i}{\partial x}, \ldots, \rho D\frac{\partial \sigma_{N-1}}{\partial x}\right)$$

$$G_2 = \left(\kappa_m \frac{\partial T}{\partial y} + \sum_i \rho D(h_i - h_N)\frac{\partial \sigma_i}{\partial y} + u\tau_{yx} + v\tau_{yy}, 0, \tau_{yx}, \tau_{yy}, \rho D\frac{\partial \sigma_i}{\partial y}, \ldots, \rho D\frac{\partial \sigma_{N-1}}{\partial y}\right)$$

$$\Omega = (0,\ 0,\ 0,\ \alpha\tau_+,\ \Sigma_k \omega_{1k} \ldots \Sigma_k \omega_{(N-1)k}). \tag{1}$$

The shear stress terms are given by,

$$\tau_{xx} = 2\mu_m \frac{\partial u}{\partial x} - \frac{2}{3}\mu_m \left(\frac{\partial u}{\partial x} + \frac{\partial v}{\partial y} + \frac{v\alpha}{y}\right) \tag{2}$$

$$\tau_{yy} = 2\mu_m \frac{\partial v}{\partial y} - \frac{2}{3}\mu_m \left(\frac{\partial u}{\partial x} + \frac{\partial v}{\partial y} + \frac{v\alpha}{y}\right) \tag{3}$$

$$\tau_{xy} = \tau_{yx} = \mu_m \left(\frac{\partial u}{\partial y} + \frac{\partial v}{\partial x} + \frac{v\alpha}{y}\right) \tag{4}$$

$$\tau_+ = 2\mu_m \frac{v\alpha}{y} - \frac{2}{3}\mu_m \left(\frac{\partial u}{\partial x} + \frac{\partial v}{\partial y} + \frac{v\alpha}{y}\right) \tag{5}$$

In these equations, σ_i and ω_i are the mass fraction and chemical production term for the i-th species, respectively. The species viscosity (μ) and thermal conductivity (κ) are referenced to μ_o, κ_o , and T_{o_κ} using Sutherland's law,

$$\frac{\mu_i}{\mu_{oi}} = \left(\frac{T}{T_{o\mu}}\right)^{3/2} \frac{T_{o\mu} + S_\mu}{T + S_\mu} \quad , \quad \frac{\kappa_i}{\kappa_{oi}} = \left(\frac{T}{T_{o\kappa}}\right)^{3/2} \frac{T_{o\kappa} + S_\kappa}{T + S_\kappa} \quad , \tag{6}$$

where T_{o_μ}, T_{o_κ}, S_μ, and S_κ vary with species (see Stull and Prophet 1971). The mixture viscosity and thermal conductivity are determined using Wilke's law (Wilke 1950) denoting f as μ or κ,

$$f_m = \sum_{i=1}^{N} \frac{X_i f_i}{\sum_{j=1}^{N} X_j \phi_{ij}} \tag{7}$$

$$\phi_{ij} = \frac{1}{\sqrt{8}} \left(1 + \frac{M_i}{M_j}\right)^{-1/2} \left[1 + \left(\frac{f_i}{f_j}\right)^{1/2} \left(\frac{M_j}{M_i}\right)^{1/4}\right]^2 \quad , \tag{8}$$

where X_i and M_i are the mole fraction and molecular weight of the i-th species, respectively. Fick's law is used to relate the mixture diffusivity to the mixture viscosity through the Schmidt number $Sc = \mu_m/(\rho D)$. The specific heat, enthalpy, and Gibbs free energy of each species (per mass) are given by the following fourth-order temperature (T) polynomial curve fits (Drummond, Rogers, and Hussaini 1987) (ΔH_{fi} is the heat of formation and R_i is the specific gas constant for the i-th species).

$$\frac{c_{pi}}{R_i} = A_i + B_i T + C_i T^2 + D_i T^3 + E_i T^4 \tag{9}$$

$$h_i = R_i\left(A_i + \frac{B_i}{2}T + \frac{C_i}{3}T^2 + \frac{D_i}{4}T^3 + \frac{E_i}{5}T^4\right)T + \Delta H_{fi} \tag{10}$$

$$\frac{g_i}{R_i} = A_i(T - T\ln T) - \frac{B_i}{2}T^2 - \frac{C_i}{6}T^3 - \frac{D_i}{12}T^4 - \frac{E_i}{20}T^5 + \frac{\Delta H_{fi}}{R_i} - F_iT\ . \tag{11}$$

The mixture enthalpy, total energy per unit volume, and ratio of specific heats are given by

$$h = \sum_{i=1}^{N} \sigma_i \int^T c_{pi} dT + \sum_{i=1}^{N} \sigma_i \Delta H_{fi} \tag{12}$$

$$e = \frac{p}{\gamma - 1} + \rho\frac{(u^2+v^2)}{2} + \sum_{i=1}^{N} \rho\sigma_i \Delta H_{fi} \tag{13}$$

$$\gamma = 1 + \frac{1}{\dfrac{c_{pm}}{R_u \sum_i (\sigma_i/M_i)} - 1} \tag{14}$$

$$c_{pm} = \frac{1}{T}\sum_{i=1}^{N} \sigma_i \int^T c_{pi}\, dT\ . \tag{15}$$

A covolume equation of state is used to relate pressure (p) to temperature (T).

$$p(V - b) = nR_uT, \qquad b = \sum_{i=1}^{N} n_i b_i\ , \tag{16}$$

where V is the volume, b is the covolume (Hirshfelder, Curtiss, and Bird 1954), n is the number of moles of gas, and R_u is the universal gas constant.

The system of Navier-Stokes equations in equation 1 is valid for the laminar flow of a viscous Newtonian fluid. In reality, the flow will remain laminar up to a certain critical value of the Reynolds number, $\rho UL/\mu$, where U and L are representative values of the velocity and length. Above this critical value the flow becomes turbulent and is characterized by the appearance of fluctuations in all variables (U, p, ρ, T, etc.) around mean values. These fluctuations are statistical in nature and cannot be described in a deterministic way. In this investigation, the Reynolds-averaging approximation is used along with algebraic turbulence models that relate fluid viscosity (μ) to other variables. See Nusca (1993) for further details.

Hydrocarbon mixtures such as $3CH_4 + 2O_2 + 10N_2$, pressurized to 50–100 atm, are commonly used for ram accelerator testing at ARL. A single test can incorporate several different gas mixtures in different sections of the accelerator tube, separated by diaphragms. Fuel-rich mixtures are used with fuel equivalence ratios as high as 3. For these conditions, a good understanding of CH_4/O_2 chemical kinetics, especially for $P \geq 10$ atm, is not available (Anderson and Kotlar 1991). Accurate numerical simulation of hydrocarbon-based reacting flow is very demanding in terms of computational resources since the number of intermediate species and the number of kinetic steps are prohibitively large (i.e., ≥15). For high-pressure systems, the computational investment may not be justified due to uncertainty in measured reaction kinetics. Thus, global reaction mechanisms (neglecting intermediate steps) such as

$$\begin{aligned} CH_4 + 2O_2 &\Leftrightarrow CO + 2H_2 + 1.5O_2 \\ CO + 0.5O_2 &\Leftrightarrow CO_2 \\ 2H_2 + O_2 &\Leftrightarrow 2H_2O \end{aligned} \tag{17}$$

have been used. The reaction rate is defined using the Law of Mass Action and an Arrhenius expression for C, the specific reaction rate constant.

$$\omega = C\prod_{i=1}^{N} \sigma_i^{\nu_i} = AT^{\alpha}\exp\left(\frac{-E_a}{R_u T}\right)\sigma_{CH_4}^{a}\sigma_{O_2}^{b}\sigma_{CO}^{c}\alpha_{H_2}^{d}\sigma_{CO_2}^{e}\sigma_{H_2O}^{f}\,, \tag{18}$$

where AT^{α} is the collision frequency, the exponential term is the Boltzmann factor, E_a is the activation energy, and ν_i represents the stoichiometric coefficient. Exponents a–f are chosen such that the reaction rates match results from flame experiments using large kinetic mechanisms (Westbrook and Dryer 1981) and are given by Nusca (1993).

An Arrhenius reaction rate may not be correct for the high-pressure flows, and much of the necessary reaction rate data for hydrocarbon fuels has not been measured above 10 atm (Westbrook and Dryer 1981). In addition, the three-step kinetics mechanism described previously (Eq. 18) is based on the low-pressure studies of Westbrook (Westbrook and Dryer 1981) where the exponents are determined by matching experimentally measured flame speed. For the ARL full-bore ram accelerator, where mixture ignition is largely determined by shock-induced (i.e., reflected shocks from the accelerator tube wall) and viscous heating, the exponents a–f were altered to the degree necessary to match accelerator tube wall pressures measured at ARL (Nusca 1991, 1993, 1994; Kruczynksi and Nusca 1992). It was found that ram accelerator performance was determined to a large degree by the reaction induction length (i.e., ignition delay time), which is a function of scale and mixture (as well as pressure). For the preliminary CFD computations described in the present report, no attempt has been made to alter the kinetic steps or the reaction rate expression for the subbore projectile that uses ignition via a step on the projectile. Experimental confirmation of mixture ignition (i.e., location, extent, and resulting tube wall pressure history) is required to validate the kinetics model used in the CFD code. However, the code has been extensively validated for high-speed compressible gas dynamics (Palaniswamy, Ota, and Chakravarthy 1991).

An additional issue that must be resolved is turbulence modeling. No attempt has been made in the present work (or that described by Nusca [1994] for the ARL projectile) to test the dependence of results on various models of turbulence. Nusca (1993) has documented the effects of viscosity for the full-bore projectile and has achieved good results using algebraic turbulence models. No attempt has been made in the present applications to alter these models.

3. RESULTS AND DISCUSSION

Figure 2 shows the computational mesh for the projectile with a step located at the forebody-midbody junction, 1 mm in height. The forebody is conical, 85.1 mm in length with cone half-angle 10°. The midbody is cylindrical, 30 mm in length, and 32 mm in diameter. The afterbody is conical, 98.6 mm in

length, and with a half-angle of 3.5°. The grid was generated in zones so that sharp body junctions are accurately represented. Approximately 11,000 grid cells cover the projectile and 600 grid cells reside in the wake (for the half-plane).

A gas mixture of $3CH_4 + 2O_2 + 10N_2$ was used for the CFD simulations described in this section. The mixture is characterized by a frozen speed of sound a = 361 m/s, ratio of specific heats $\gamma = 1.376$, and a Chapman-Jouget detonation velocity V_{CJ} = 1,450 m/s. The initial pressure and temperature of the mixture (before projectile injection) was 50 atm and 300 K, respectively.

Figure 3 shows the computed frozen flow Mach number contours in grey-scale (bright white represents zero value, i.e., the projectile, while dark black represents a value of about 6) for the projectile geometry displayed in Figure 2 (step height of 1 mm) and a freestream Mach number of 6 (V = 2,175 m/s, V/V_{CJ} = 1.5). This calculation (as are all calculations described in this report) was performed assuming steady-state conditions. Important gas dynamic features are labeled. A bow shock extends from the projectile nose, while the step produces a normal shock and a small stagnation region. The merging of these shocks produces a curved "transmitted shock" (Figure 1) that reflects from the accelerator tube wall, downstream of the projectile. Behind the transmitted shock, a contact surface is formed (not fully visible in Mach number contours) that separates flows of different density, temperature and velocity (i.e., flow having passed through different shock waves). The recirculation zone behind the projectile (wake) is clearly subsonic. The results for a freestream Mach number of 10 (V = 3,610 m/s, V/V_{CJ} = 2.5), displayed in Figure 4, show a downstream bending of the bow and transmitted shocks as well as a strengthening (i.e., producing lower values of the downstream Mach number flow, greyer color) of the transmitted shock and step-generated normal shock.

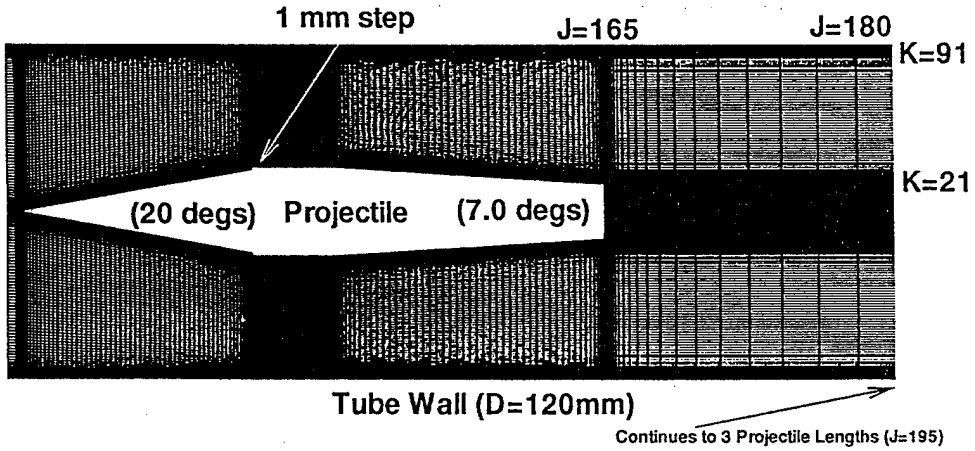

Figure 2. Computational mesh. Projectile with 1-mm step.

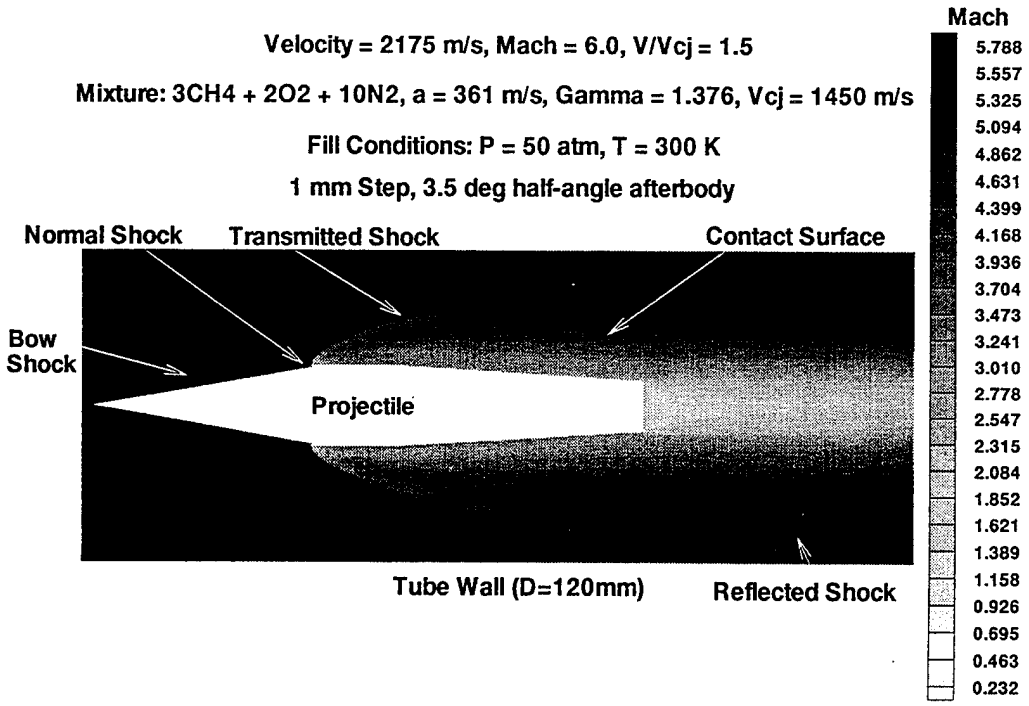

Figure 3. Nonreacting Mach number contours, freestream Mach no. 6, 1-mm step.

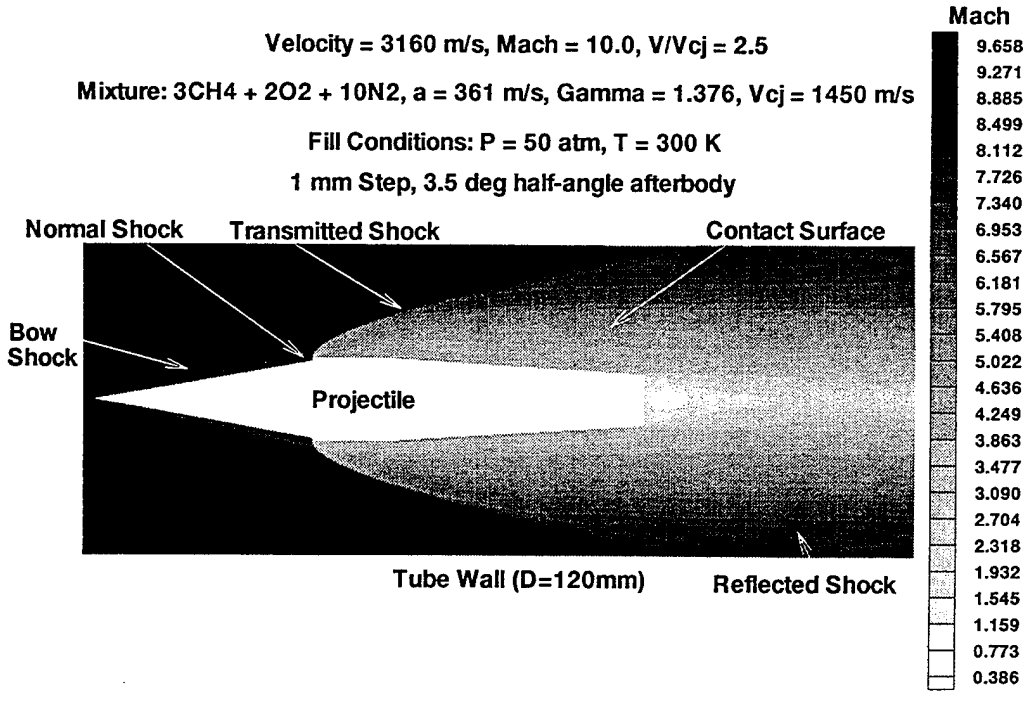

Figure 4. Nonreacting Mach number contours, freestream Mach no. 10, 1-mm step.

Figures 5, 6, and 7 show water (H_2O is a major product of the combustion) mass fraction contours in grey-scale (bright white representing the absence of water and dark black representing a mass fraction of 0.07 and above). These calculations are an extension of the steady-state results shown in Figures 3 and 4 with the flow now allowed to chemically react. Figures 6 and 7 are closer views of the step region. Major combustion activity is predicted, using the current kinetics mechanism (Eq. 17), in the step-generated stagnation region (behind the normal shock) and continuing around the step and then over the projectile surface. This region of strong combustion and combustion products effectively resides between the contact surface and the projectile surface. The projectile wake flow entrains combustion products. Note in Figure 6 that the production of H_2O is reduced somewhat (i.e., lighter grey colors) after expansion around the step, but is not extinguished. Figure 6 also shows a close view of the same step height but at a freestream Mach number of 10. The H_2O mass fraction distribution is more uniform and extends farther into the flowfield radially away from the projectile.

The bow shock wave from the nose does not initiate chemical reaction. The detached normal shock wave ahead of the step initiates a very strong detonation wave that intersects the bow shock. At the intersection point, a transmitted shock is directed towards the tube wall. The strength of this transmitted shock depends on the flow Mach number and step height. The transmitted shock weakens as its distance from the projectile increases, until reaching the tube wall and reflecting. At the intersection point between the bow shock and the detonation wave, ahead of the step, a contact-combustion surface is also generated. This contact surface begins at the intersection point, which is a few step heights above the surface, and is propagated from there nearly parallel to the projectile surface towards the projectile base and further downstream, above the wake. The temperature of the flow with combustion products, behind the step, is about 5 to 8 times the freestream temperature, and the pressure is about 10 to 15 times the freestream pressure. This contact surface separates the hot flow of the combustion products, processed by the detonation ahead of the step, and the outer flow that passed through the transmitted shock wave. Therefore, the contact surface acts as an aerodynamic cowling, while the region between the contact surface and the projectile body surface acts in a manner similar to a combustion chamber in a conventional ramjet engine. However, the "combustion chamber" is confined by the aerodynamic contact surface without requiring the structural cowling of a conventional engine. The high-pressure, high-temperature combustion products in this aerodynamic "combustion chamber" can then be expanded over the projectile afterbody to produce thrust.

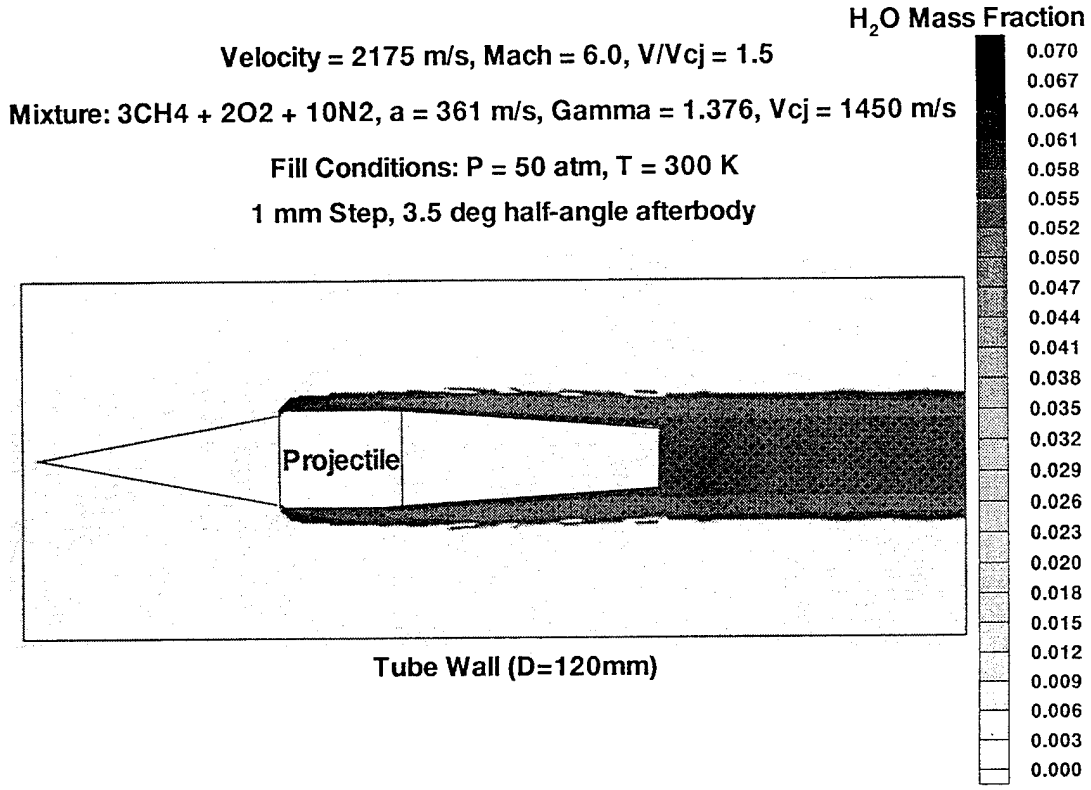

Figure 5. Reacting H_2O contours, freestream Mach no. 6, 1-mm step.

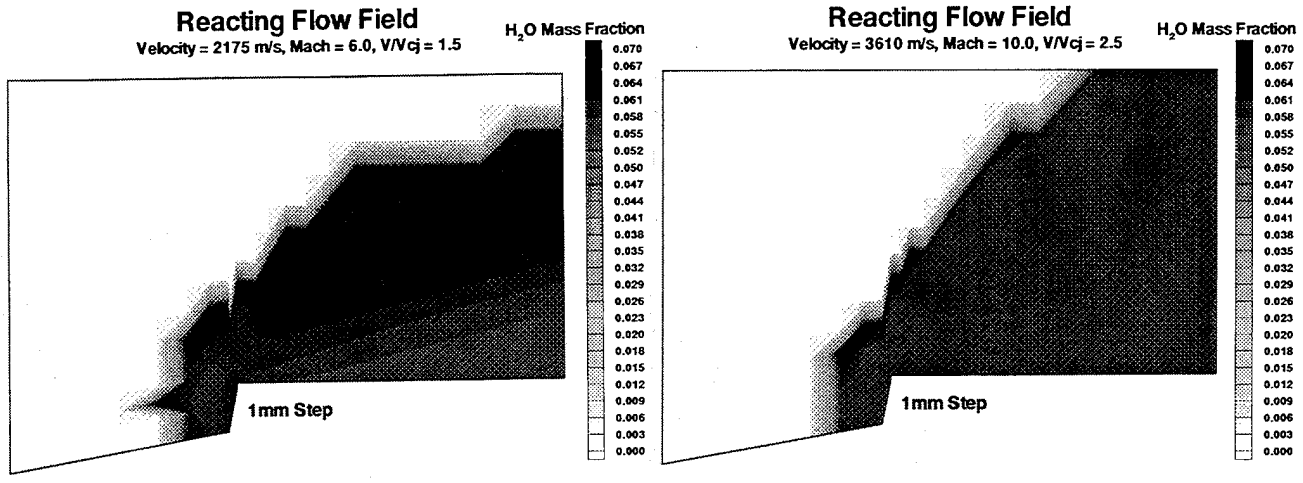

Figure 6. Reacting H_2O contours, freestream Mach nos. 6 and 10, 1-mm step.

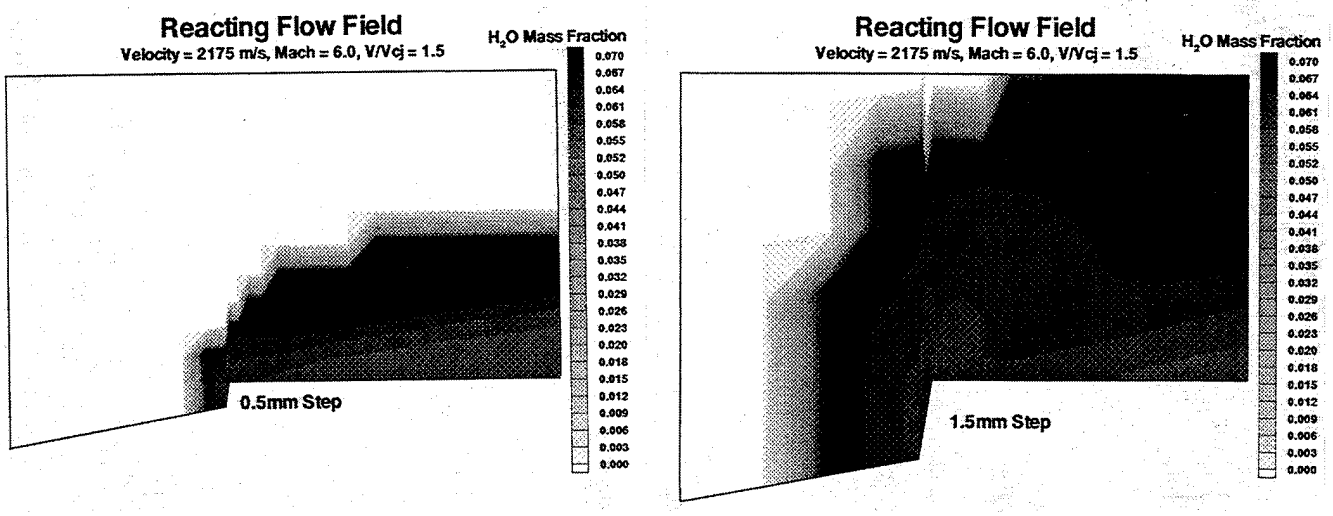

Figure 7. Reacting H_2O contours, freestream Mach no. 6, 0.5- and 1.5-mm steps.

Figure 7 shows water mass fraction contours in the vicinity of the 0.5- and 1.5-mm steps for a freestream Mach number of 6. The H_2O mass fraction distributions are similar to those for the 1-mm step height, but with the combustion region remaining close to the projectile body for the 0.5-mm step and extending farther into the flowfield for the 1.5-mm step. The larger step causes a more extensive stagnation region in front of the step (behind the normal shock).

As the step height is increased, the conditions and the position of the contact surface are effected, resulting in increased mass of combustion products at higher pressures and temperatures, but with an increase in drag due the increased step height. The observation that combustion can be initiated and sustained for the 0.5-mm step is in general agreement with the approximate analysis of Rom and Avital (1992) where the minimum step height for establishing a combustion-detonation front ahead of a step for stoichiometric CH_4/O_2 mixture is evaluated. This step height is about 0.7 mm for Mach no. 6 and precombustion pressure of 1 atmosphere.

The computed pressure distributions on the projectile surface were integrated to form a thrust coefficient, F/PA, where P is the initial mixture pressure (50 atm) and A is the cross-sectional area of the accelerator tube (diameter of 120 mm). For a freestream Mach number of 6 and the 1-mm step, the nonreacting flow yielded F/PA = –0.4 (i.e., drag), while the reacting flow yielded F/PA = 3.1. Projectiles with step heights of 0.5 mm and 1.5 mm, and nonreacting flow yielded F/PA = –0.3 and –0.9, respectively. With chemical reactions, these cases yielded F/PA = 3.4 and 3.06, respectively. The 0.5-mm

step yields a smaller drag that must be canceled by the thrust produced by combustion and thus yields a larger thrust coefficient. The 1.5-mm step yields a larger drag that must be canceled by the thrust produced by combustion. Nevertheless, the more extensive combustion for this step height yields a positive thrust.

The author feels confident about the fidelity of the CFD code with regards to gas dynamic phenomena displayed in this section. However, the accuracy of the assumed chemical kinetics mechanism can be argued, especially at high-pressure and fuel-rich conditions. Further research and validation is warranted. The presented results should therefore be considered preliminary.

4. CONCLUSIONS

The present numerical simulation of the effects of a forward-facing step positioned on the body of a hypervelocity projectile, clearly indicates that the step will produce chemical reactions of the hydrocarbon atmosphere. The present calculations also show that these reactions do not extinguish after flow expansion around the step, are sustained over the afterbody and the wake of the projectile, and can be used to produce thrust. It is shown that the interaction between the bow shock from the conical forebody and the detached shock-detonation wave from the forward-facing step, which is positioned on the shoulder of the projectile, results in confinement of a combustion layer about the projectile afterbody. The high-pressure and temperature products of the combustion, which are confined to this layer, are then expanded into the rear and the base flow of the projectile and can be used to generate thrust. However, since the projectile shape and combustion scales are different in the present external propulsion case from those in the Ram Accelerator case, these results should be validated by an experimental firing of the projectile geometry investigated.

5. REFERENCES

Anderson, W. R., and A. J. Kotlar. "Detailed Modeling of CH_4/O_2 Combustion for Hybrid In-Bore Ram Propulsion (HIRAM) Application." 28th JANNAF Combustion Meeting, Brooks Air Force Base, San Antonio, TX, 28 October–1 November 1991.

Chakravarthy, S. R., K. Y. Szema, U. C. Goldberg, J. J. Gorski, and S. Osher. "Application of a New Class of High Accuracy TVD Schemes to the Navier-Stokes Equations." AIAA-85-0165, Proceedings of the AIAA 23rd Aerospace Sciences Meeting, Reno, NV, 14–17 January 1985.

Drummond, J. P., C. Rogers, and M. Y. Hussaini. "A Numerical Model for Supersonic Reacting Mixing Layer." Computer Methods in Applied Mechanics and Engineering, vol. 64, 1987.

Giraud, M., J-F. Legendre, and G. Simon. "Ram Acceleration at ISL; First Experiments in 90mm Caliber." Proceedings of the 42nd Meeting of the Aeroballistic Range Association, Adelaide, Australia, pp. 12–16, 1991.

Hertzberg, A., A. P. Bruckner, and D. W. Bogdanoff. "Ram Accelerator: A New Chemical Method for Accelerating Projectiles to Ultrahigh Velocities." AIAA Journal, vol. 26, no. 2, pp. 195–103, 1988.

Hirschfelder, J. O., C. F. Curtiss, and R. Bird. Molecular Theory of Gases and Liquids. New York: John Wiley and Sons, 1954.

Kruczynski, D. L., and M. J. Nusca. "Experimental and Computational Investigation of Scaling Phenomena in a Large Scale Ram Accelerator." AIAA-92-3245, Proceedings of the 28th AIAA/SAE/ASME/ASEE Joint Propulsion Conference, Nashville, TN, 6–8 July 1992.

Nusca, M. J. "Numerical Simulation of Reacting Flow in a Thermally Choked Ram Accelerator Projectile Launch System." AIAA-91-2490, Proceedings of the 27th AIAA/SAE/ASME/ASEE Joint Propulsion Conference, Sacramento, CA, 24–26 June 1991.

Nusca, M. J. "Numerical Simulation of Fluid Dynamics with Finite-Rate and Equilibrium Combustion Kinetics for the 120-mm Ram Accelerator." AIAA-93-2182, Proceedings of the 29th AIAA/SAE/ASME/ASEE Joint Propulsion Conference, Monterey, CA, 29–30 June 1993.

Nusca, M. J. "Reacting Flow Simulation for a Large Scale Ram Accelerator." AIAA-94-2963, Proceedings of the 30th AIAA Joint Propulsion Conference, Indianapolis, IN, 27–29 June 1994.

Palaniswamy, S., and S. R. Chakravarthy. "Finite Rate Chemistry for USA Series Codes: Formulation and Applications." AIAA-89-0200, Proceedings of the 27th AIAA Aerospace Sciences Meeting, Reno, NV, 9–12 January 1989.

Palaniswamy, S., D. K. Ota, and S. R. Chakravarthy. "Some Reacting-Flow Validation Results for USA-Series Codes." AIAA-91-0583, Proceedings of the 29th AIAA Aerospace Sciences Meeting, Reno, NV, 7–10 January 1991.

Roe, P. L. "Approximate Riemann Solvers, Parameter Vectors, and Difference Schemes." Journal of Computational Physics, vol. 43, pp. 357–372, 1981.

Rom, J. "Method and Apparatus for Launching a Projectile at Hypersonic Velocity." U.S. Patent 4,932,306, 12 June 1990.

Rom, J., and Y. Kivity. "Accelerating Projectiles up to 12 km/sec Utilizing the Continuous Detonation Propulsion Method." AIAA Paper No. 88-2969, 1988.

Rom, J., and G. Avital. "The External Propulsion Accelerator: Scramjet Thrust Without Interaction With the Accelerator Barrel." AIAA Paper No. 92-3717, 1992.

Smeets, G., F. Seiler, G. Patz, and J. Srulijes. "First Results Obtained in a 30mm Caliber Scram Accelerator Using a Rail Tube For Cylindrical Projectiles." Proceedings of the 25th International Symposium on Combustion, Irvine, CA, pp. 21–35, 1994.

Stull, D. R., and H. Prophet. JANNAF Thermochemical Tables. 2nd ed., National Bureau of Standards, NSRDS-Rept. 37, June 1971.

Westbrook, C. K., and F. L. Dryer. "Simplified Reaction Mechanisms for the Oxidation of Hydrocarbon Fuels in Flames." Combustion and Science Technology, vol. 27, pp 31–43, 1981.

Wilke, C. R. "A Viscosity Equation for Gas Mixtures." Journal of Chemistry and Physics, vol. 18, no. 4, pp. 517–519, 1950.

LIST OF SYMBOLS

A	cross-sectional area of launch tube
b	covolume
c_p	specific heat capacity, constant p
c_v	specific heat capacity, constant volume
C	specific reaction rate constant
D	mass diffusion coefficient
e	specific total internal energy
E_a	activation energy
F,G	flux vectors (Eq. 1)
g	Gibbs energy per mole
h	molar specific enthalpy
i	i-th species
L	total body length
m	mixture quantity
M	molecular weight
n	number of moles
N	total number of species
p	static pressure
R	specific gas constant, $(\gamma\text{-}1)c_p/\gamma$
R_u	universal gas constant, RM_m
Re	Reynolds number, $\rho UL/\mu$
Sc	Schmidt number, $\mu_m/\rho D$
t	time
T	static temperature
u	axial velocity
v	radial velocity
U	magnitude of the local velocity vector
V	specific volume $(1/\rho)$
W	dependent variable vector (Eq. 1)
x,y	cartesian coordinates
X	species mole fraction

α	0 for 2D, 1 for axisymmetric
γ	ratio of specific heats, c_p/c_v
ΔH_f	enthalpy of formation
κ	heat transfer coefficient
μ	molecular viscosity
ν	stoichiometric coefficient
ρ	density
σ	species mass fraction
τ	shear stress tensor
ω	chemical production term (Eq. 18)
Ω	source term vector (Eq. 1)

NO. OF COPIES	ORGANIZATION
2	ADMINISTRATOR DEFENSE TECHNICAL INFO CTR ATTN DTIC DDA CAMERON STATION ALEXANDRIA VA 22304-6145
1	DIRECTOR US ARMY RESEARCH LAB ATTN AMSRL OP SD TA 2800 POWDER MILL RD ADELPHI MD 20783-1145
3	DIRECTOR US ARMY RESEARCH LAB ATTN AMSRL OP SD TL 2800 POWDER MILL RD ADELPHI MD 20783-1145
1	DIRECTOR US ARMY RESEARCH LAB ATTN AMSRL OP SD TP 2800 POWDER MILL RD ADELPHI MD 20783-1145
	ABERDEEN PROVING GROUND
5	DIR USARL ATTN AMSRL OP AP L (305)

NO. OF COPIES	ORGANIZATION
2	HQDA ATTN SARD TR MS K KOMINOS DR R CHAIT WASHINGTON DC 20310-0103
1	SDOP TNI ATTN L H CAVNEY PENTAGON WASHINGTON DC 20301-7100
6	COMMANDER USA ARDEC ATTN SMCAR AET A R DEKLEINE R KLINE R BOTTICELLIE H HUDGINS J GRAU S KAHN PICATINNY ARSENAL NJ 07806-5001
1	COMMANDER USA ARDEC ATTN SMCAR CCH V P VALENTI PICATINNY ARSENAL NJ 07806-5001
1	COMMANDER US ARMY RESEARCH OFFICE ATTN TECHNICAL LIBRARY PO BOX 12211 RESEARCH TRIANGLE PARK NC 27709-2211
1	COMMANDER US ARMY RESEARCH OFFICE ATTN D MANN PO BOX 12211 RESEARCH TRIANGLE PARK NC 27709-2211
1	DIRECTOR US ARMY RESEARCH OFFICE ATTN AMXRO MCS K CLARK PO BOX 12211 RESEARCH TRIANGLE PARK NC 27709-2211
1	DIRECTOR US ARMY RESEARCH OFFICE ATTN AMXRO RT IP LIBRARY SERVICES PO BOX 12211 RESEARCH TRIANGLE PARK NC 27709-2211

NO. OF COPIES	ORGANIZATION
1	COMMANDER NAVAL RESEARCH LABORATORY ATTN TECHNICAL LIBRARY WASHINGTON DC 20375-5000
3	COMMANDER NAVAL RESEARCH LABORATORY ATTN CODE 4410 K KAILASANATH J BORIS E ORAN WASHINGTON DC 20375-5000
1	COMMANDER NAVAL SURFACE WARFARE CENTER ATTN DR F MOORE DAHLGREN VA 22448
7	COMMANDER NAVAL SURFACE WARFARE CENTER ATTN T C SMITH K RICE S MITCHELL S PETERS J CONSAGA C GOTZMER TECHNICAL LIBRARY INDIAN HEAD MD 20640-5000
2	COMMANDER NSWC WHITE OAK LABS ATTN CODE R44 DR A WARDLAW K24 B402 12 DR W YANTA SILVER SPRING MD 20903-5000
1	USAF WRIGHT AERONAUTICAL LABS ATTN AFWAL FIMG DR J SHANG WRIGHT PATTERSON AFB OH 45433-6553
1	AFOSR NA ATTN J TISHKOFF BOLLING AFB 20332-6448
3	AIR FORCE ARMAMENT LABORATORY ATTN AFATL FXA S C KORN B SIMPSON S BELK EGLIN AFB FL 32542-5434

NO. OF COPIES	ORGANIZATION
2	WL MNSH ATTN R DRABCZUK D LITTRELL EGLIN AFB FL 32542-5434
1	LOS ALAMOS NATIONAL LABORATORY ATTN B HOGAN MS G770 LOS ALAMOS NM 87545
2	DIRECTOR SANDIA NATIONAL LABORATORIES ATTN DIV 1554 DR W OBERKAMPF DIV 1554 DR F BLOTTNER ALBUQUERQUE NM 87185
4	DIRECTOR NASA LANGLEY RESEARCH CENTER ATTN TECH LIBRARY D M BUSHNELL DR M J HEMSCH DR J SOUTH LANGLEY STATION HAMPTON VA 23665
2	DIRECTOR NASA LANGLEY RESEARCH CENTER ATTN MS 408 W SCALLION D WITCOFSKI HAMPTON VA 23605
1	DIRECTOR NASA AMES RESEARCH CENTER ATTN MS 227 8 L SCHIFF MOFFETT FIELD CA 94035
5	DIRECTOR NASA AMES RESEARCH CENTER ATTN MS 258 1 D CHAUSSEE MS 258 1 T HOLST MS 258 1 P KUTLER MS 258 1 P BUNING MS 258 1 M RAI MOFFETT FIELD CA 94035
1	UNITED STATES MILITARY ACADEMY DEPARTMENT OF MECHANICS ATTN LTC ANDREW L DULL WEST POINT NY 10996

NO. OF COPIES	ORGANIZATION
1	UNIVERSITY OF CALIFORNIA DAVIS DEPT OF MECHANICAL ENGINEERING ATTN PROF H A DWYER DAVIS CA 95616
1	MASSACHUSETTS INST OF TECH ATTN TECH LIBRARY 77 MASSACHUSETTS AVE CAMBRIDGE MA 02139
1	VA POLYTECHNIC INST & STATE UNIV DEPT OF AEROSPACE & OCEAN ENGRG ATTN DR C H LEWIS BLACKSBURG VA 24061
1	ADVANCED TECH CTR ARVIN CALSPAN AERODYNAMICS RESEARCH DEPT ATTN DR M S HOLDEN PO BOX 400 BUFFALO NY 14225
1	THE PENNSYLVANIA STATE UNIVERSITY DEPT OF AEROSPACE ENGRG ATTN DR G S DULIKRAVICH UNIVERSITY PARK PA 16802
3	THE PENNSYLVANIA STATE UNIVERSITY DEPT OF MECHANICAL ENGRG ATTN V YANG K KUO C MERKLE UNIVERSITY PARK PA 16802-7501
1	UNIVERSITY OF ILLINOIS AT URBANA CHAMPAIGN DEPT OF MECHANICAL & INDUSTRIAL ENGRG ATTN DR J C DUTTON URBANA IL 61801
3	UNIVERSITY OF MARYLAND DEPT OF AEROSPACE ENGINEERING ATTN DR J D ANDERSON JR DR W MELNIK DR M LEWIS COLLEGE PARK MD 20742
1	UNIVERSITY OF NOTRE DAME DEPT OF AERONAUTICAL & MECHANICAL ENGRG ATTN PROF T J MUELLER NOTRE DAME IN 46556

NO. OF COPIES	ORGANIZATION
1	UNIVERSITY OF TEXAS DEPT OF AEROSPACE ENGRG MECHANICS ATTN DR D S DOLLING AUSTIN TX 78712-1055
1	UNIVERSITY OF DELAWARE DEPT OF MECHANICAL ENGRG ATTN DR J MEAKIN CHAIRMAN NEWARK DE 19716
3	SCIENCE AND TECHNOLOGY INC ATTN D MAURIZI B LOLTMAN A GLASSER 4001 N FAIRFAX DR NO 700 ARLINGTON VA 22203-1618
1	GRUMANN AEROSPACE CORPORATION AEROPHYSICS RESEARCH DEPARTMENT ATTN DR R E MELNIK BETHPAGE NY 11714
1	AEDC CALSPAN FIELD SERVICE ATTN MS 600 DR J BENEK TULLAHOMA TN 37389
1	ARROW TECHNOLOGY ASSOC INC ATTN W HATHAWAY PO BOX 4218 SOUTH BURLINGTON VT 05401-0042
1	PAUL GOUGH ASSOCIATES INC ATT P S GOUGH 1048 SOUTH ST PORTSMOUTH NH 03801-5423
2	PRINCETON COMBUSTION RESEARCH LABS INC ATTN N MER N A MESSINA PRINCETON CORP PLAZA 11 DEERPARK DR BLDG IV STE 119 MONMOUTH JUNCTION NJ 08852
1	ROCKWELL INTERNATIONAL ROCKETDYNE DIVISION ATTN BA08 R B EDELMAN 6633 CANOGA AVE CANOGA PARK CA 91303-2703
1	ROCKWELL INTERNATIONAL SCIENCE CTR ATTN DR S PALANISWAMY 1049 CAMINO DOS RIOS THOUSAND OAKS CA 91360
1	VERITAY TECHNOLOGY INC ATTN E FISHER 4845 MILLERSPORT HWY EAST AMHERST NY 14501-0305
1	META COMP TECHNOLOGIES INC ATT S CHAKRAVARTHY 650 WESTLAKE BLVD SUITE 203 WESTLAKE VILLAGE CA 91362
	ABERDEEN PROVING GROUND, MD
33	DIR, USARL ATTN: AMSRL-WT-P, A. HORST AMSRL-WT-PB, E. SCHMIDT B. GUIDOS P. PLOSTINS J. SAHU P. WEINACHT G. COOPER AMSRL-WT, R. FIFER AMSRL-WT-PD, B. BURNS AMSRL-WT-PA, T. MINOR M. NUSCA 7 CPS G. WREN T. COFFEE J. DESPIRITO D. KOOKER D. KRUCZYNSKI G. KELLER F. LIBERATORE P. CONROY W. OBERLE AMSRL-WT-W, C. MURPHY AMSRL-WT-WB, W. D'AMICO AMSRL-WT-NC, R. LOTERRO AMSRL-CI-C, W. STUREK C. NEITUBICZ D HISLEY

USER EVALUATION SHEET/CHANGE OF ADDRESS

This Laboratory undertakes a continuing effort to improve the quality of the reports it publishes. Your comments/answers to the items/questions below will aid us in our efforts.

1. ARL Report Number ARL-TR-920 Date of Report January 1996

2. Date Report Received _____

3. Does this report satisfy a need? (Comment on purpose, related project, or other area of interest for which the report will be used.) _____

4. Specifically, how is the report being used? (Information source, design data, procedure, source of ideas, etc.) _____

5. Has the information in this report led to any quantitative savings as far as man-hours or dollars saved, operating costs avoided, or efficiencies achieved, etc? If so, please elaborate. _____

6. General Comments. What do you think should be changed to improve future reports? (Indicate changes to organization, technical content, format, etc.) _____

CURRENT ADDRESS

_____
Organization

_____
Name

_____
Street or P.O. Box No.

_____
City, State, Zip Code

7. If indicating a Change of Address or Address Correction, please provide the Current or Correct address above and the Old or Incorrect address below.

OLD ADDRESS

_____
Organization

_____
Name

_____
Street or P.O. Box No.

_____
City, State, Zip Code

(Remove this sheet, fold as indicated, tape closed, and mail.)
(DO NOT STAPLE)